Equilibrium between Quenched and Nonquenched Conformations of the Major Plant Light-Harvesting Complex Studied with High-Pressure Time-Resolved Fluorescence

Bart van Oort,[†] **Arie van Hoek,**[†,§] **Alexander V. Ruban,**[‡] **and Herbert van Amerongen*,**[†,§]

Laboratory of Biophysics, Wageningen University, Dreijenlaan 3, 6703HA Wageningen, The Netherlands, School of Biological and Chemical Sciences, Queen Mary University of London Mile End, Bancroft Road, London E1 4NS, United Kingdom, and Microspectroscopy Centre Wageningen, Dreijenlaan 3, 6703HA Wageningen, The Netherlands

Nonphotochemical quenching (NPQ) of chlorophyll fluorescence plays an important role in the protection of plants against excessive light. Fluorescence quenching of the major light-harvesting complex (LHCII) provides a model system to study the mechanism of NPQ. The existence of both quenched and nonquenched states of LHCII has been postulated. We used time-resolved fluorescence and hydrostatic pressure to study differences between these states. Pressure shifts the thermodynamic equilibrium between the two states. The estimated volume difference was 5 mL/mol, indicating a local conformational switch. The estimated free energy difference was 7.0 kJ/mol: high enough to keep the quenched state population low under normal conditions, but low enough to switch in a controlled way. These properties are physiologically relevant properties, because they guarantee efficient light harvesting, while at the same time maintaining the capacity to switch to a quenched state. These results indicate that conformational changes of LHCII can play an important role in NPQ.

Introduction

Photosynthesis provides a large input into the global food chain by converting solar energy into chemical energy. Primary reactions of this process take place in the thylakoid membrane, where a number of protein complexes are organized to conduct the photon energy conversion into the energy of ATP and NADPH. The photosynthetic systems are organized as supercomplexes: reaction centers are surrounded by antennae. The antennae consist of several pigment–protein complexes containing large amounts of photochemically inactive pigments, which greatly enhance the effective reaction center absorption cross section. This enables plant growth at very low light intensity. However, the light intensity can fluctuate greatly during a day (up to hundreds of times). Too much light can be damaging, particularly for photosystem II, which carries one of the greatest oxidizers in nature, reaction center P680, capable of removing electrons from water, using it as fuel for driving the photosynthetic electron transport.[1] In order to avoid potentially lethal damage to the membrane by the "great oxidizer", a mechanism of NPQ is employed.[2] NPQ responds to frequent variations in light intensity, working as a safety valve to reduce the excitation pressure in photosystem II.

NPQ is a well-controlled and heterogeneous process. It consists of qE and qI. qE is rapidly reversible in the dark and is triggered by an increase in the ΔpH across the photosynthetic membrane. qI has slower recovery kinetics and can appear as photoinhibition, which may actually be due to a photoprotective mechanism.[3] Three known major factors, ΔpH across the photosynthetic membrane, the xanthophyll cycle carotenoid, zeaxanthin, and PSII protein, PsbS, determine the magnitude

and kinetic properties of NPQ.[3,4] Despite a long history of NPQ research, neither the molecular mechanism nor its control is well-understood. It is currently one of the major topics in the increasingly multidisciplinary field of photosynthesis research.[5] Two of the key mechanistic questions regarding qE are as follows: how is the transition into the photoprotective mode occurring, and what is the physical nature of the energy dissipation process — the quencher's identity? Protonation of LHCII proteins is currently considered a major qE event, triggering a conformational transition in antenna into a dissipative, photoprotective state.[6] The NPQ-associated events in LHCII antenna have been the focus of a number of important recent studies.[7–12] Most of them agree that a conformational change within the LHCII system is behind the *mechanics* of the process. It has been suggested that qE is the result of a protonation-induced conformational change in the LHCII antenna associated with the promotion of protein–protein association leading to aggregation (for a recent review, see ref 6). Isolated LHCII has been found to dissipate excitation energy very efficiently, reproducing closely the main qE features.[13,14] The extent of this aggregation was found to be controlled by the xanthophyll cycle carotenoids in such a manner that, while violaxanthin inhibits aggregation, zeaxanthin promotes it, causing amplification in energy quenching.[13,14] These observations led to the further development of an allosteric model for NPQ, where protonation-triggered LHCII aggregation caused changes in chlorophyll–chlorophyll or chlorophyll–carotenoid interactions in the antenna, leading to the formation of energy dissipating pairs of pigments.[6]

Recently, we obtained the first direct evidence that the conformational state of the LHCII trimer tunes its biological function by altering the configuration of bound pigments.[15] The structural model of this complex, as determined by X-ray crystallography,[16] was found to be that of the photoprotective or dissipative antenna state because of the 5 times reduced

---
* Phone: +31 317 485200; fax: +31 317 482725; e-mail: bart.vanoort@wur.nl.
† Wageningen University.
‡ Queen Mary University of London Mile End.
§ Microscopy Centre Wageningen.

chlorophyll excited state/fluorescence lifetime. Because of a particular order of trimers in the crystal, the likelihood of formation of abnormal pigment interactions leading to the quenched state, as was frequently argued,[17] was excluded. A group of long-wavelength low-temperature fluorescence bands and specific Raman features arising from the neoxanthin-Chl *b* domain were detected in crystals; these were similar to those reported earlier for quenched LHCII aggregates, but with greatly enhanced spectral resolution arising because of the high uniformity of protein conformation in the crystal.

The fluorescence decay of various LHCII preparations was often found to be biexponential, with the major part of the decay in ~4 ns, and a small fraction decaying with 0.3−2 ns.[18−20] These two lifetimes are likely to arise from LHCII in different conformations,[18,19] supporting the idea of the existence of a conformational switch. In this work, we use high hydrostatic pressure to shift the thermodynamic equilibrium in order to estimate volume and free energy differences between the two postulated states.

We show that a conformational switch of LHCII does exist and leads to the quenching. We provide the thermodynamic analysis of this transition. The quenched state is present to a small extent in isolated LHCII (few percent) and becomes more populated under high hydrostatic pressure. The switch is associated with a small volume difference, indicating a local switch. The associated energy difference is high enough to keep the population of the quenched state low under standard conditions, but the difference is low enough to easily populate it under favoring conditions.

Experimental Methods

Sample Preparation. Trimeric LHCII was isolated from maize plants (*Zea mays* L. cv. LG11) of approximately two weeks old, using the method of Caffari et al.[21] Samples were stored at −70 °C in 0.5 M sucrose and measured within 6 months after isolation. For all experiments, the samples were diluted at least 100-fold in sucrose-free medium (0.06% β-DM (Inalco S.p.A., Milan, Italy), 10 mM Hepes (Sigma, MO)), which is a pressure-independent pH buffer,[22] pH 7.5, to an OD of less than 0.05 at 435 nm. As a reference experiment, the concentrated sample was diluted in 5% Triton X-100 (Pharmacia, Uppsala, Sweden). This leads to complete uncoupling of pigments (see results, and, e.g., ref 23). This sample is named "uncoupled LHCII". All buffers were prepared with ultrapure water (MilliQ gradient A10, Millipor, MA). The Chl *a/b* ratio was 1.33, and the Chl/Xan ratio was 4.1, as determined by deconvolution of the absorption spectra of the 80% acetone extract with the spectra of the individual pigments[24] (a refinement of the method of Porra et al.[25]).

High-Pressure Fluorescence Measurements. Steady-state fluorescence spectra were recorded on a Spex-Fluorolog 3.2.2 spectrofluorimeter (Jobin-Yvon Horiba). For emission spectra, excitation was at 435 nm. For excitation spectra, detection was at 681 nm with trimeric LHCII and at 675 nm with uncoupled LHCII. Slit widths were 0.5 nm (excitation) and 5 nm (detection) in order to reduce photodegradation while maintaining sufficient detection sensitivity.

Fluorescence decay curves were recorded by time-correlated single photon counting (TCSPC) as described elsewhere.[26] In brief, the samples were excited with vertically polarized 435 nm wavelength light pulses of 0.2 ps duration at a repetition rate of 3.8 MHz, with typically 100 nW average power (annihilation free). Fluorescence was collected at a right angle with respect to the exciting light beam and at magic angle

TABLE 1: Main Results of Steady-State and Time-Resolved Fluorescence Experiments: Shift of Emission Maximu (dν/dP), Relative Fluorescence Quantum Yield Change with Pressure (dφ_f/dP), and Fluorescence Quantum Yield at 400 MPa Relative to that at 0.1 MPa (φ_f^{400MPa})^a

	trimeric LHCII	uncoupled LHCII
dν/dp (cm^{-1}/MPa)^b	-0.118 (0.011)	-0.160 (0.019)
dφ_f/dp (%/MPa)^b	-0.093 (0.003)	-0.121 (0.004)
dφ_f/dp (%/MPa)^c	-0.023 (0.001)	-0.0115 (0.0005)
dφ_f/dp (%/MPa)^d	-0.091 (0.005)	e
φ_f^{400MPa} (%)^b	0.623 (0.007)	0.516 (0.009)
φ_f^{400MPa} (%)^c	0.910 (0.004)	0.954 (0.002)
φ_f^{400MPa} (%)^d	0.638 (0.017)	e

^{a} Values result from linear fits of ν and φ_f vs pressure. Standard errors calculated from the fits are in parentheses. ^{b} From steady-state fluorescence. ^{c} From two-component fit of fluorescence decay. ^{d} From three-component fit of fluorescence decay. ^{e} A third component was not detected.

polarization, through a 665 nm long wave pass filter (Schott). Fluorescence decay data were stored in 4096 channels of a multichannel analyzer (5.0 ps time spacing). The instrument response function (~30 ps fwhm) was obtained with pinacyanol iodide in methanol (10 ps fluorescence lifetime). Decay traces were fitted to a sum of exponentials, with home-built software.[27]

The fluorescence setups were equipped with a high-pressure cell (ISS Inc./APP). Samples were in a 6×6 mm^2 quartz cuvette sealed with plastic foil and placed in the ethanol (spectroscopic grade, Merck) bath which was then pressurized. Pressure was increased in 12 evenly spaced steps from atmospheric pressure to 400 MPa. At each pressure, the samples were equilibrated for at least 5 min prior to measurements. All experiments were performed at 287 K.

Results

Steady-State Fluorescence. We measured fluorescence emission and excitation spectra of LHCII trimers in micelles at various hydrostatic pressures. As a reference, we studied LHCII in which all pigments were uncoupled by 5% Triton X-100 (detection at 675 nm: mostly Chl *a*). The main results are summarized in Table 1 and Figures 1−3. The quenching and spectral shift of fluorescence upon pressure variation were reversible within the accuracy of the experiment.

At 435 nm mostly Chl *a* and a small amount of Xan and Chl *b* are excited.[28] In the intact complex, excitation energy on Xan and Chl *b* is rapidly transferred to Chl *a*;[29] therefore, almost all fluorescence originates from Chl *a*. In the uncoupled complexes, no energy transfer occurs, so both Chl *a* and *b* fluorescence can be observed. Fluorescence detected from Chl *b* is roughly 95% weaker than that from Chl *a* because of (i) selective Chl *a* excitation, (ii) selective detection of Chl *a*, (iii) lower concentration of Chl *b*, and (iv) lower fluorescence quantum yield of Chl *b*.[30]

A selection of emission spectra is given in Figure 1. All spectra are corrected for concentration changes due to compression of the solvent[31] and for changes in the absorption at the excitation wavelength by a shift of the absorption bands due to the applied pressure. Such a correction, with the use of excitation spectra, is straightforward, because the shape of the 435 nm absorption band does not change significantly upon shifting (based on the excitation spectra; results not shown).

The fluorescence yield decreases with increasing pressure: 0.093%/MPa for trimeric LHCII and 0.121%/MPa for uncoupled LHCII (Figure 2, Table 1). The emission spectra shift to the red: 0.118 cm^{-1}/MPa for trimeric LHCII and 0.160 cm^{-1}/MPa for uncoupled LHCII (free pigments in ethanol showed similar

Equilibrium between Quenched and Nonquenched LHCII

J. Phys. Chem. B, Vol. 111, No. 26, 2007 **7633**
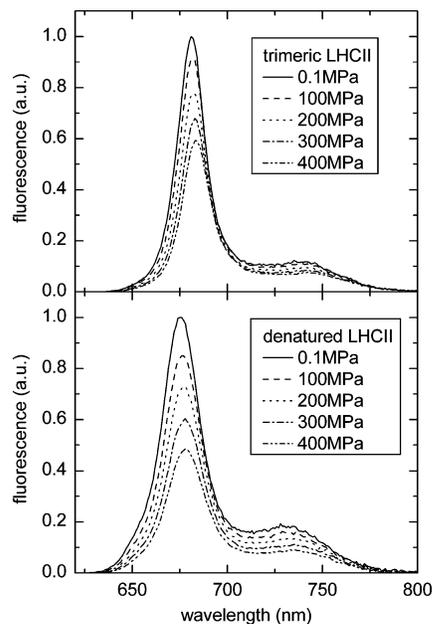
Figure 1. Fluorescence emission spectra of trimeric (upper) and uncoupled LHCII (5% Triton X-100), at 283 K at different pressures. Spectra were recorded at 33 MPa intervals; for clarity, not all spectra are shown.
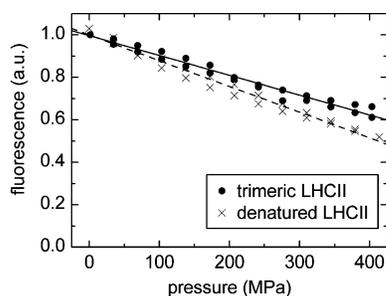
Figure 2. Integrated fluorescence emission intensity of trimeric and uncoupled LHCII at different pressures, with linear fit (line and dashed line; see also Table 1). Data were obtained at increasing and decreasing pressure, with 5 min equilibration time at each pressure.

results). The fluorescence quenching and shift resemble those induced by aggregation, although high pressure does not lead to aggregation (see ref 32 and discussion).

Fluorescence excitation spectra are sensitive to changes in absorption spectra and changes in energy transfer among different pigment molecules.[33] Therefore, changes of excitation spectra provide information on conformational changes. Both in the Chl and in the Xan regions the spectra change. Difference spectra are also shown in Figure 3: spectra at 400 MPa minus 0.1 MPa. The spectra were first normalized on the area of the Soret region. A large fraction of the change appeared due to a shift of the Chl spectra. Therefore, difference spectra were also calculated from a 400 MPa spectrum that was shifted such that the peak at 435 nm overlapped with the 0.1 MPa spectrum.

The fluorescence excitation spectrum of uncoupled LHCII shows no sign of energy transfer from Chl *b* or Xan to Chl *a*, so all pigments are uncoupled. The difference spectrum constructed from the "aligned" 400 MPa spectrum resembles a Chl *b* minus Chl *a* spectrum. So, (1) for free Chl, the absorption bands shift, and (2) relatively less Chl *a* fluorescence is detected at high pressure. Observation (2) is not due to a relative decrease of the Chl *a* fluorescence quantum yield (see discussion), but due to a red-shift of the emission spectra, which leads to a relative decrease of Chl *a* fluorescence at the detection wavelength (675 nm).
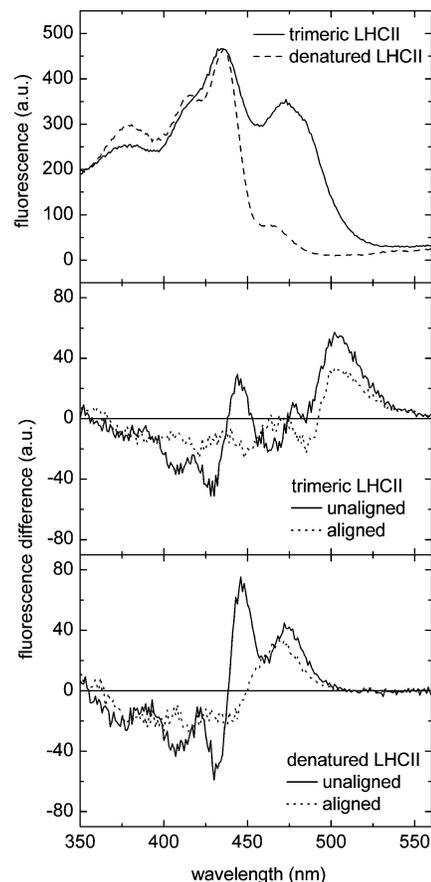
Figure 3. Fluorescence excitation spectra of trimeric LHCII (detection at 681 nm) and uncoupled LHCII (detection at 675 nm) at 0.1 MPa (upper), and fluorescence excitation difference spectra (400 − 0.1 MPa) of trimeric LHCII (middle) and uncoupled LHCII (lower). Difference spectra were calculated after normalizing the area of the Soret region of the spectra. Difference spectra calculated from spectra that were aligned on the 435 nm peak are shown in dotted lines.

The fluorescence excitation spectrum of trimeric LHCII also shifts. The difference spectrum contructed from the "aligned" 400 MPa spectrum (3.8 nm blue-shifted) shows a decrease in the Chl *a* (375−450 nm) and the Chl *b*/neoxanthin (488 nm) regions, and an increase at 505 nm.

Time-Resolved Fluorescence. The quenching process(es) were further studied by time-correlated single photon counting (TCSPC). Each fluorescence decay trace was fitted by a sum of exponentials. At each pressure the sum of pre-exponential factors (amplitudes) was normalized. For trimeric LHCII, both the amplitudes and the lifetimes depend on pressure, whereas for uncoupled LHCII, this is only the case for the lifetimes. The decay times change approximately linearly with pressure. The main TCSPC results are summarized in Table 1 and in Figure 4.

The fluorescence quantum yield at pressure *p* relative to the value at atmospheric pressure is given by eq 1, provided that the two fitted lifetimes are the only ones present in the sample.

$$\varphi_f^p = \frac{a_1^p \tau_1^p + a_2^p \tau_2^p}{a_1^0 \tau_1^0 + a_2^0 \tau_2^0} \tag{1}$$

In eq 1, a_n^p and τ_n^p are the amplitude and lifetime of component *n* at pressure *p*; *p* = 0 indicates atmospheric pressure.

First, we present the TCSPC results on LHCII trimers. The fluorescence decay is described very well with two lifetimes: $\tau_1 = \sim 0.5$ ns (very small amplitude) and $\tau_2 = \sim 3.5$ ns. This
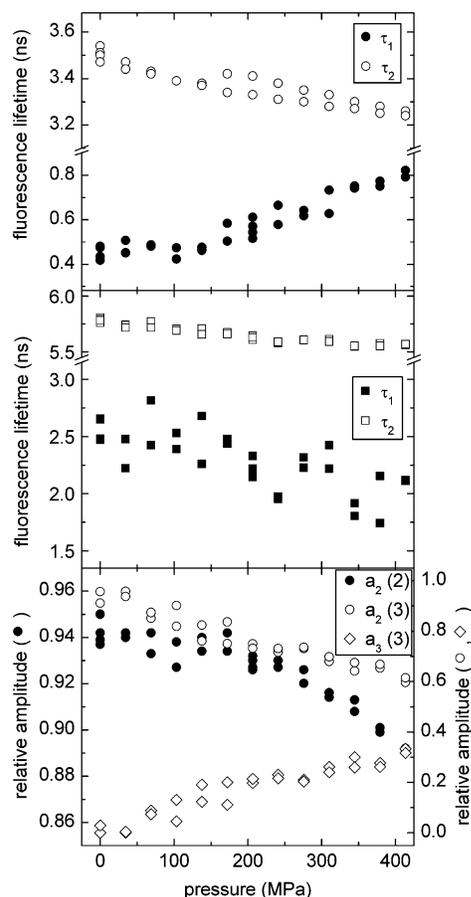
Figure 4. Fit results of fluorescence decay: lifetimes of trimeric LHCII (upper) and uncoupled LHCII (middle). The relative amplitudes of two-component ($a_2(2)$) and three-component ($a_2(3)$ and $a_3(3)$) fits for trimeric LHCII are in the lower panel. At each pressure, the sum of amplitudes equals unity (including amplitude 1, not shown). The lifetimes are the results of two-component fits and are identical to those of the fit with an additional (25 ± 9 ps) component. The relative amplitudes of uncoupled LHCII were independent of pressure; $a_1 = 0.101$ (standard error: 0.008) and $a_2 = 0.899$ (standard error: 0.008).

agrees with previous experiments, e.g., Palacios et al.[20] τ_1 slightly increases and τ_2 slightly decreases upon increasing the pressure. The relative fluorescence yield at 400 MPa is 0.91, according to eq 1; however, the steady-state experiments give a value of 0.62 (Figure 2). Thus, a two-component description of the system is incomplete: an additional fluorescence decay path must be present.

The additional decay path must be fast or else the quality of the two-component fits would have been bad. To resolve the third lifetime (τ_3), we fitted decay traces at all pressures globally: τ_3 was forced to be equal at all pressures, while all other parameters ($a^p_{1,2,3}$, $\tau^p_{1,2}$) were not restricted.

An additional lifetime was now resolved: $\tau_3 = 25$ ps. The other lifetimes and the ratio a_2/a_1 hardly change. The amplitude a_3 represents the relative concentration of a strongly quenched fraction of LHCII. The concentration increases from 0% at atmospheric pressure to 31% at 400 MPa. The relative fluorescence yield is 0.64, as calculated from eq 1 extended to three lifetimes. This yield is identical (within the errors; see Table 1) to that of the steady-state experiments.

Second, we present the TCSPC results on uncoupled LHCII. The fluorescence decay curves contain two lifetimes: ~2 ns (Chl *b*) and ~5.7 ns (Chl *a*) (lifetime attribution with ref 30). Both lifetimes decrease with increasing pressure (Figure 4). The corresponding amplitudes do not change. The total fluorescence

at 400 MPa is 95% relative to that at atmospheric pressure as calculated according to eq 1; however, the steady-state experiments give 52%.

The remaining 43% of fluorescence quenching must be caused by ultrafast quenching of a large fraction of the Chls. Global analysis did not resolve an additional decay path. Therefore, the lifetime should be shorter than the time resolution (~5−10 ps).

If an addional fluorescence lifetime component exists, and this component is not present at atmospheric pressure, then the relative quantum yield is given by eq 2. With $\varphi^{400MPa}_f = 1 -$

$$\varphi^p_f = \frac{a^p_1\tau^p_1 + a^p_2\tau^p_2 + a^p_3\tau^p_3}{a^0_1\tau^0_1 + a^0_2\tau^0_2} \qquad (2)$$

$0.49 = 0.51$ and using $\tau_3 \leq 10$ ps, it follows that $a^{400MPa}_3 \approx 0.47$. So, in uncoupled LHCII, 47% of all Chl is in a strongly quenched state at 400 MPa. The relative amplitudes of Chl *a* and *b* do not depend on pressure. So, fluorescence quenching is equally strong for Chl *a* and *b*.

Discussion

Fluorescence Excitation Spectra. The fluorescence excitation difference spectrum of trimeric LHCII at 400 MPa minus 0.1 MPa shows a decrease in the Chl *a* region and the Chl *b*/neoxanthin region (~488 nm) and an increase at 505 nm (Figure 3). It is remarkable that *in vivo* quenching is accompanied by an absorption increase at 505 nm, which is usually ascribed to de-epoxidation of violaxanthin into zeaxanthin.[34] In our sample, such a de-epoxidation does not take place, and the increase is most likely due to a red-shift of one (or more) of the carotenoids. However, we cannot be sure that the spectral change is directly related to the fluorescence quenching.

The 25 ps Fluorescence Lifetime of Trimeric LHCII. The fluorescence quenching of trimeric LHCII upon increasing pressure from atmospheric to 400 MPa is 37%. 26% of the quenching is due to the formation of a 25 ps decay path. The fraction of LHCII trimers with this fluorescence lifetime increases from 0% to 31% when the pressure increases from atmospheric pressure to 400 MPa. Our experiments do not give information on the nature of the quenching species. We used very low excitation power (<0.1 pJ per pulse, 3.8 MHz repetition rate), so the 25 ps decay is not due to singlet−singlet or singlet−triplet annihilation.

One strongly quenched Chl can quench all the fluorescence of an LHCII trimer. The time needed for an excitation on an arbitrary pigment within the trimer to reach a quencher is expected to be on the order of the spatial excitation equilibration time. This time was estimated to be 48 ps in trimeric LCHII and 32 ps in trimeric units within aggregated LHCII.[35] Thus, it seems likely that the 25 ps lifetime reflects the time for an excitation to reach a single quenching site in a trimer. This means that, with 42 Chls per trimer,[16] less than 1% of all Chls are highly quenched, whereas in uncoupled LHCII, 47% of all Chls are highly quenched. The possible role of this quenching *in vivo* will be discussed below.

The ~0.5 ns Component Is Not Caused by Aggregation. Several arguments plead against the ~0.5 ns component originating from aggregates of LHCII: (1) The changes in the absorption spectra due to pressure are identical in LHCII in agarose gel (no aggregation) and under high detergent concentration.[32] (2) The fluorescence quenching is the same in LHCII in agarose gel and in micelles.[32] (3) The aggregation-dependent
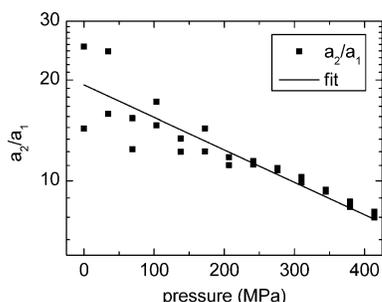
Figure 5. Ratio a_2/a_1 from the three-lifetime analysis of time-resolved fluorescence of trimeric LHCII fitted with eq 4. See text for more details.

scatter does not change (Figure 3 and ref 32). (4) The fluorescence lifetime of the ~0.5 ns component increases with pressure, whereas the lifetimes of aggregates decrease (results not shown). (5) The change of relative amplides of the various decay paths was completely reversible in trimeric LHCII, and not in aggregates (results not shown).

The Longer Fluorescence Lifetimes of Trimeric LHCII. What do the two major fluorescence lifetimes of trimeric LHCII mean? Moya et al.,[19] and later Huyer et al.,[18] correlated two lifetimes to two conformations of the LHCII, one of which might function as a sink for excess light energy and the other as an efficient light harvester. Some studies found single-exponential fluorescence decay,[20,35] and the number of lifetimes seems to depend on sample preparation.[36] The pressure dependence of the amplitudes of the lifetimes provides additional information.

Suppose the two lifetimes correspond to two distinct conformations of LHCII. The concentration (proportional to $a_{1,2}$) of each conformation depends on pressure (Figure 4). An increase in pressure favors reduction of the volume of a system. If higher-order terms are neglected with respect to pressure, the Gibbs free energy difference between two states (ΔG_{12}) is a linear function of pressure (eq 3),

$$\Delta G_{12} = -RT \ln K_{12} = \Delta G_{12}^0 + p\Delta V_{12} \qquad (3)$$

where ΔG_{12}^0 is the standard Gibbs free energy difference (at 0.1 MPa (1 bar), 297 K); ΔV_{12} the partial molar volume difference between the two states; R the gas constant; T temperature; p pressure; and K_{12} the equilibrium constant governing the process. Thus, in an equilibrium of two conformations, K_{12} depends on pressure as eq 4.

$$K_{12}(p) = \frac{a_2(p)}{a_1(p)} = e^{-\left(\Delta G_{12}^0 + p\Delta V_{12}\right)/RT} = c_1 \times e^{-c_2 p}$$

with constants, between $c_1 = e^{-(\Delta G_{12}^0)/RT}$ and $c_2 = \Delta V_{12}/RT$

$$c_1 = e^{-(\Delta G_{12}^0)/RT} \qquad c_2 = \frac{\Delta V_{12}}{RT} \qquad (4)$$

We obtained a good fit of the ratio of amplitudes to eq 4 (Figure 5), with $\Delta G_{12}^0 = -7.0$ (0.3) kJ/mol and $\Delta V_{12} = 5.3 \times 10^{-6}$ (1.5 $\times$ 10^{-6}) m^3/mol or 8.8 $\times$ 10^{-3} (2.5 $\times$ 10^{-3}) nm^3/trimer (values in parentheses indicate 95% confidential intervals). The volume of trimeric LHCII is approximately 150 nm^3, as calculated from the LHCII crystal structures of spinach[16] and pea,[17] using *SwissPdbViewer* (v. 3.7). The relative volume difference between the two conformations is thus 0.006%. This small structural difference relates well with the very small

structural changes observed during quenching by detergent removal (without aggregation).[37]

How does this volume difference relate to the protein compression at 400 MPa? Typical values for the protein compressibility (κ) are in the range 0.05–0.15 GPa^{-1}.[38] The spectral shift of chromophores in solution depends on pressure according to eq 5, which emerges from the theory of Laird and Skinner.[39]

$$\Delta\nu/\Delta p = n\kappa 3^{-1}(\nu_m - \nu_{vac}) \qquad (5)$$

$\Delta\nu/\Delta p$ is pressure shift of the absorption maximum (in wavenumbers per GPa); κ compressibility, ν_m frequency of the absorption maximum at atmospheric pressure, ν_{vac} frequency of the optical transition in vacuum (=15 551 cm^{-1} for Chl a[40]), and the attractive chromophore–solvent interaction (E) depends on the intermolecular distance R as $E = $ constant $\times R^n$. Although this equation describes chromophores in solution, it was proven to apply for photosynthetic complexes, provided the Chls are well-separated, with weak electrostatic couplings and with small charge-transfer-state effects.[41] This is the case for LHCII.[42−44]

The compressibilty of LHCII at 77 K is 0.045 GPa^{-1}, as calculated from the shift of the absorption maximum at 676.1 nm,[43] using eq 5. The shift at 287 K is probably several tens of percent higher than at 77 K.[45] Next, we will estimate the LHCII compressibility from our data.

If we assume that the pressure shift of the Chl a absorption maximum is roughly equal to the shift of the emission maximum, the compressibility at 287 K is 0.08 GPa^{-1} (with $\nu_m = 675$ nm, $\Delta\nu/\Delta p = -0.012$ cm^{-1}/MPa). This assumption is not entirely correct: after absorption, the excitation energy redistributes over the Chls a, with different absorption maxima. These maxima, between 664.9 and 683.3 nm,[46] correspond to compressibilities between 0.12 and 0.06 GPa^{-1}. Most of the fluorescence originates from the red Chls, which indicate a compressibility of 0.06−0.08 GPa^{-1}. This compares well with the value calculated from the 77 K absorption spectra. We conclude that LHCII compression is approximately 3% at 400 MPa.

Thus, the volume difference between the two conformations (ΔV_{12}) is much smaller (0.006%) than the LHCII volume difference between atmospheric pressure and 400 MPa (~3%). This suggests that ΔV_{12} may depend on pressure, which would explain the slight deviation between our data and the fit with eq 4 (Figure 5). Nevertheless, eq 4 still describes the data fairly well. This has some implications.

First, the amplitudes behave according to the thermodynamical description of a two-state system. So, the two fluorescence lifetimes represent two states, i.e., two different protein conformations, in agreement with results from low-temperature time-resolved fluorescence.[18,19] Moreover, the results show that these states are in a dynamic equilibrium.

Second, the two conformations are quite resistant to pressure: the volume decrease due to pressure exceeds the volume difference between the conformations 500-fold, yet there remain two distinct conformations (the conformations maintain distinct fluorescence lifetimes). Apparently, the pressure-induced volume changes affect mainly other conformational properties than those that form the difference between the two conformations identified by the two lifetimes. It points to a local conformational change with a volume change that is much smaller than the overall volume change upon compression.

Several processes can lead to a volume difference on the order of ΔV_{12} (5 mL/mol) and an energy difference of ΔG_{12}^0 (−7.0 kJ/mol), for example, hydrogen bond formation and solvation of singly charged ions.[47] Cis−trans isomerization of

a carotenoid can also lead to a similar volume change, e.g., in bacteriorhodopsin;[48] however, the free energy change of this reaction is 59 kJ/mol,[49] much higher than our ΔG_{12}. It should be noted that, in contrast with LHCII, in bacteriorhodopsin the chromophore is covalently bound to the protein. Bending of a carotenoid would probably lead to a smaller volume and energy change than isomerization. Raman spectroscopy showed two major difference between nonquenched LHCII trimers in micelles and quenched LHCII crystals: bending of the neoxanthin and hydrogen bonding of at least one Chl *b*.[15] Lampoura et al. demonstrated changes in the Chl−Car interaction upon aggregation,[50] and Wentworth et al. correlated the transition of LHCII from an nonquenched to a quenched state with a perturbation in the Lut 1 region.[37] Although LHCII crystals are in a quenched state,[15] most spectroscopic data on (nonquenched) trimeric LHCII can be explained by the crystal structure.[51] All these observations are in agreement with the small volume and energy differences we measure.

The Nature of the Quenchers/Quenching *in Vivo*? Aggregation of LHCII leads to fluorescence quenching (see, e.g., ref 52) and may play a role in NPQ.[53] Different mechanisms have been suggested to explain this quenching: It could be caused either by (i) a small population of strongly quenched LHCIIs, that also quench fluorescence of connected LHCII (e.g.[52]), or (ii) by conformational changes of a large fraction of LHCII, thereby less strongly quenching fluorescence of each LHCII (e.g., ref 6). From our results, we cannot conclude which mechanism is the most likely one: the fluorescence quenching is due both to the formation of quenched species ($\tau = 25$ ps) and to conformational switching of LHCII between two conformations with different quenching rates. The energy difference between these two conformations is small, and therefore the quenched conformation may be stabilized by environmental changes (such as pH, membrane structure, aggregation) induced by high light intensities.

Conclusions

We have shown the following: (i) Pressure creates a quenching species in trimeric LHCII. The lifetime of quenched trimers is 25 ps, which reflects the excitation equilibration time or, in other words, the time to reach an ultrafast quencher somewhere within the trimer. (ii) The fluorescence of uncoupled LHCII, and thus of individual chromophores, is far more susceptible to quenching than the chlorophylls in trimeric LHCII (approximately 50-fold). (iii) The two longer fluorescence lifetimes of trimeric LHCII originate from two protein conformations. These conformations are in a dynamic equilibrium, which is shifted by pressure. The volume difference between the two conformations is 5 mL/mol, or 0.006%, pointing to a local conformational switch between a quenched and an nonquenched trimer. This volume difference is in agreement with the small structural differences between nonquenched LHCII in micelles and quenched LHCII crystals.[15] We cannot be sure that a similar way of quenching also occurs in vivo. It has recently been argued that the structure of the LHCII trimer in detergent is not identical to the structure in the thylakoid membrane.[54] However, our measurements show that such a change can readily occur in LHCII. The rapid quencher (25 ps) could also be physiologically relevant. It can only be present in few LHCII trimers, to prevent quenching that is too strong.

Thus, it appears that within LHCII the Chls are organized such that they are not susceptible to random, uncontrolled quenching. It should be noted that reconstituted and monomeric LHCII always show a higher degree of quenching, and the

organization appears to be less "perfect".[36,37] At the same time, different conformations exist with different fluorescence yields, and the difference in free energy between them is high enough to keep the quenched-state population low under normal conditions, but low enough (much lower than the energy of a photon) to switch in a controlled way. These properties guarantee efficient light harvesting, while at the same time maintaining the capacity to switch to a quenched state, possibly a physiologically relevant quenching one. These results indicate that conformational changes of LHCII can play a role in NPQ *in vivo*.

References and Notes

(1) Barber, J. *Aust. J. Plant Physiol.* **1995**, *22*, 201−208.

(2) Horton, P.; Ruban, A. V.; Walters, R. G. *Annu. Rev. Plant Physiol. Plant Mol. Biol.* **1996**, *47*, 655−684.

(3) Niyogi, K. K. *Annu. Rev. Plant Physiol. Plant Mol. Biol.* **1999**, *50*, 333−359.

(4) Demmig-Adams, B. *Biochim. Biophys. Acta.* **1990**, *1020*, 1−24.

(5) van Oort, B. F.; Ruban, A. V.; van Hoek, A.; van Amerongen, H. In *13th International Congress of Photosynthesis*; van der Est, A., Bruce, D., Eds.; Alliance Communications Group, Kansas, U.S.A., Montreal, Canada, 2004; Vol. 1, p 142−144.

(6) Horton, P.; Wentworth, M.; Ruban, A. V. *FEBS Lett.* **2005**, *579*, 4201−4206.

(7) Aspinall-O'Dea, M.; Wentworth, M.; Pascal, A.; Robert, B.; Ruban, A. V.; Horton, P. *Proc. Natl. Acad. Sci. U.S.A.* **2002**, *99*, 16331−16335.

(8) Bassi, R.; Caffarri, S. *Photosynth. Res.* **2000**, *64*, 243−256.

(9) Holt, N. E.; Zigmantas, D.; Valkunas, L.; Li, X.-P.; Niyogi, K. K.; Fleming, G. R. *Science* **2005**, *307*, 433−436.

(10) Horton, P.; Ruban, A. V.; Wentworth, M. *Philos. Trans. R. Soc. Lond., Ser. B Biol. Sci.* **2000**, *355*, 1361−1370.

(11) Li, X.-P.; Gilmore, A. M.; Caffarri, S.; Bassi, R.; Golan, T.; Kramer, D.; Niyogi, K. K. *J. Biol. Chem.* **2004**, *279*, 22866−22874.

(12) Ruban, A. V.; Pascal, A. A.; Robert, B.; Horton, P. *J. Biol. Chem.* **2002**, *277*, 7785−7789.

(13) Ruban, A. V.; Horton, P. *Plant Physiol.* **1999**, *119*, 531−542.

(14) Ruban, A. V.; Young, A.; Horton, P. *Biochim. Biophys. Acta* **1994**, *1186*, 123−127.

(15) Pascal, A. A.; Liu, Z. F.; Broess, K.; van Oort, B.; van Amerongen, H.; Wang, C.; Horton, P.; Robert, B.; Chang, W. R.; Ruban, A. *Nature* **2005**, *436*, 134−137.

(16) Liu, Z. F.; Yan, H.; Wang, K.; Kuang, T.; Zhang, J.; Gui, L.; Chang, W. *Nature* **2004**, *428*, 287−292.

(17) Standfuss, J.; Terwisscha van Scheltinga, A. C.; Lamborghini, M.; Kühlbrandt, W. *EMBO J.* **2005**, *24*, 919−928.

(18) Huyer, J.; Eckert, H.-J.; Irrgang, K.-D.; Miao, J.; Eichler, H.-J.; Renger, G. *J. Phys. Chem. B* **2004**, *108*, 3326−3334.

(19) Moya, I.; Silvestri, M.; Vallon, O.; Cinque, G.; Bassi, R. *Biochemistry* **2001**, *40*, 12552−12561.

(20) Palacios, M. A.; de Weerd, F. L.; Ihalainen, J. A.; van Grondelle, R.; van Amerongen, H. *J. Phys. Chem. B* **2002**, *106*, 5782−5787.

(21) Caffarri, S.; Croce, R.; Breton, J.; Bassi, R. *J. Biol. Chem.* **2001**, *276*, 35924−35933.

(22) Kitamura, Y.; Itoh, T. *J. Solution Chem.* **1987**, *16*, 715−725.

(23) Dall'Osto, L.; Caffarri, S.; Bassi, R. *Plant Cell* **2005**, *17*, 1217−1232.

(24) Croce, R.; Canino, G.; Ros, F.; Bassi, R. *Biochemistry* **2002**, *41*, 7334−7343.

(25) Porra, R. J.; Thompson, W. A.; Kriedemann, P. E. *Biochim. Biophys. Acta* **1989**, *975*, 384−394.

(26) Borst, J. W.; Hink, M. A.; van Hoek, A.; Visser, A. J. W. G. *J. Fluoresc.* **2005**, *15*, 153−160.

(27) Digris, A. V.; Skakoun, V. V.; Novikov, E. G.; van Hoek, A.; Claiborne, A.; Visser, A. J. W. G. *Eur. Biophys. J.* **1999**, *28*, 526−531.

(28) Croce, R.; Cinque, G.; Holzwarth, A. R.; Bassi, R. *Photosynth. Res.* **2000**, *64*, 221−231.

Equilibrium between Quenched and Nonquenched LHCII

J. Phys. Chem. B, Vol. 111, No. 26, 2007 **7637**

(29) Connelly, J. P.; Müller, M. G.; Hucke, M.; Gatzen, G.; Mullineaux, C. W.; Ruban, A. V.; Horton, P.; Holzwarth, A. R. *J. Phys. Chem. B* **1997**, *101*, 1902−1909.

(30) Seely, G. R.; Connolly, J. S. In *Light emission by plants and bacteria*; Govindjee, Amesz, J.; Fork, D. C., Eds.; Academic Press, Inc.: Orlando, 1986; p 99−133.

(31) Fine, R. A.; Millero, F. J. *J. Chem. Phys.* **1973**, *59*, 5529−5536.

(32) Connelly, J. P.; Ruban, A. V.; Horton, P. In *High Pressure Food Science, Bioscience and Chemistry*; Isaacs, N. S., Ed.; Royal Society of Chemistry: Cambridge, U.K.; 1998; pp 417−422.

(33) van Amerongen, H.; Valkunas, L.; van Grondelle, R. *Photosynthetic excitons*; World Scientific Publishing: Singapore, 2000.

(34) Yamamoto, H. Y.; Kamite, L.; Wang, Y.-Y. *Plant Physiol.* **1972**, *49*, 224−228.

(35) Barzda, V.; Gulbinas, V.; Kananavicius, R.; Cervinskas, V.; van Amerongen, H.; van Grondelle, R.; Valkunas, L. *Biophys. J.* **2001**, *80*, 2409−2421.

(36) Palacios, M. A.; Standfuss, J.; Vengris, M.; van Oort, B. F.; van Stokkum, I. H. M.; Kühlbrandt, W.; van Amerongen, H.; van Grondelle, R. *Photosynth. Res.* **2006**, *88*, 269−285.

(37) Wentworth, M.; Ruban, A. V.; Horton, P. *J. Biol. Chem.* **2003**, *278*, 21845−21850.

(38) Reddy, N. R. S.; Wu, H.-M.; Jankowiak, R.; Picorel, R.; Cogdell, R. J.; Small, G. J. *Photosynth. Res.* **1996**, *48*, 277−289.

(39) Laird, B. B.; Skinner, J. L. *J. Chem. Phys.* **1989**, *90*, 3274−3281.

(40) Renge, I. *Chem. Phys.* **1992**, *167*, 173−184.

(41) Wu, H.-M.; Rätsep, M.; Jankowiak, R.; Cogdell, R. J.; Small, G. J. *J. Phys. Chem. B* **1998**, *102*, 4023−4034.

(42) Palacios, M. A.; Caffarri, S.; Bassi, R.; van Grondelle, R.; van Amerongen, H. *Biochim. Biophys. Acta.* **2004**, *1656*, 177−188.

(43) Pieper, J.; Rätsep, M.; Jankowiak, R.; Irrgang, K.-D.; Voigt, J.; Renger, G.; Small, G. J. *J. Phys. Chem. A* **1999**, *103*, 2412−2421.

(44) van Amerongen, H.; van Grondelle, R. *J. Phys. Chem. B* **2001**, *105*, 604−617.

(45) Reddy, N. R. S.; Wu, H.-M.; Jankowiak, R.; Picorel, R.; Cogdell, R. J.; Small, G. J. *Photosynth. Res.* **1996**, *48*, 277−289.

(46) Trinkunas, G.; Connelly, J. P.; Müller, M. G.; Valkunas, L.; Holzwarth, A. R. *J. Phys. Chem. B* **1997**, *101*, 7313−7320.

(47) Mozhaev, V. V.; Heremans, K.; Frank, J.; Masson, P.; Balny, C. *Proteins: Struct., Funct., Genet.* **1996**, *24*, 81−91.

(48) Bryl, K.; Yoshihara, K. *Eur. Biophys. J.* **2002**, *31*, 539−548.

(49) Bondar, A.-N.; Fischer, S.; Suhai, S.; Smith, J. C. *J. Phys. Chem. B* **2005**, *109*, 14786−14788.

(50) Lampoura, S. S.; Barzda, V.; Owen, G. M.; Hoff, A. J.; van Amerongen, H. *Biochemistry* **2002**, *41*, 9139−9144.

(51) Novoderezhkin, V. I.; Palacios, M. A.; van Amerongen, H.; van Grondelle, R. *J. Phys. Chem. B* **2005**, *109*, 10493−10504.

(52) Mullineaux, C. W.; Pascal, A. A.; Horton, P.; Holzwarth, A. R. *Biochim. Biophys. Acta.* **1993**, *1141*, 23−28.

(53) Horton, P.; Ruban, A. V.; Rees, D.; Pascal, A. A.; Noctor, G.; Young, A. J. *FEBS Lett.* **1991**, *292*, 1−4.

(54) Lambrev, P. H.; Varkonyi, Z.; Krumova, S.; Kovacs, L.; Miloslavina, Y.; Holzwarth, A. R.; Garab, G. *Biochim. Biophys. Acta.* **2007**, In Press.